

# $\eta$ -Nucleon Scattering Length and Effective Range uncertainties.

A.M. Green\*

*Helsinki Institute of Physics, P.O. Box 64, FIN-00014 University of Helsinki, Finland*

S. Wycech<sup>†</sup>

*Soltan Institute for Nuclear Studies, Warsaw, Poland*

(July 7, 2018)

## Abstract

The coupled  $\eta N$ ,  $\pi N$ ,  $\gamma N$ ,  $\pi\pi N$  system is described by a  $K$ -matrix method. The parameters in this model are adjusted to get an optimal fit to  $\pi N \rightarrow \pi N$ ,  $\pi N \rightarrow \eta N$ ,  $\gamma N \rightarrow \pi N$  and  $\gamma N \rightarrow \eta N$  data in an energy range of about 100 MeV or so each side of the  $\eta$ -threshold. Compared with our earlier analysis, we now utilize recent Crystal Ball data. However, the outcome confirms our previous result that the  $\eta$ -nucleon scattering length ( $a$ ) is large with a value of  $0.91(6)+i0.27(2)$  fm.

PACS numbers: 13.75.-n, 25.80.-e, 25.40.V

Typeset using REVTeX

---

\*email: anthony.green@helsinki.fi

<sup>†</sup>email: wycech@fuw.edu.pl

## I. INTRODUCTION

The value of the  $\eta$ -nucleon scattering length ( $a$ ) is still uncertain, but with everyone agreeing that it is indeed attractive *i.e.*  $a > 0$ . In the literature estimates can be found ranging from Rea of  $0.3 \pm 0.05$  fm upto about  $1.0 \pm 0.1$  fm – a selection being given in Table I.

The main interest in  $a$  lies in the fact that, if the  $\eta$ -nucleon scattering amplitude in the threshold region is sufficiently attractive, then  $\eta$ -nuclear quasi-bound states may be possible. These were first suggested about 20 years ago [17,18]. Since then many articles have appeared on this subject studying different reactions in which such quasi-bound states could manifest themselves. A bound state was indeed predicted in the simplest case *i.e.* the  $\eta$ -deuteron system [19]. On the other hand, experimental studies of the  $pn \rightarrow d\eta$  cross section [20], do not indicate any such bound  $d\eta$  system [3,21,22]. In the heavier  ${}^3\text{He}$  nucleus, the  $pd \rightarrow {}^3\text{He}\eta$  reaction suggested the likelihood of such a state [7,23]. However, the first experimental attempt to discover  $\eta$ -states in larger nuclei gave a negative conclusion [24]. Another experiment is now being undertaken to check this result [25].

Unfortunately, in the absence of  $\eta$ -beams, the formation reactions are also the only source of experimental information about the  $\eta N$  scattering length. Therefore, in any discussion, it is important that as many reactions as possible are treated simultaneously. Otherwise success with one reaction may be completely nullified by failure with another.

With this in mind, in Ref. [11], the present authors carried out a simultaneous  $K$ -matrix fit to the  $\pi N \rightarrow \eta N$  cross sections reviewed by Nefkens [26] and the  $\gamma p \rightarrow \eta p$  data of Krusche *et al.* [27]. In addition, the fit included  $\pi N$  amplitudes of Arndt *et al.* [28], since the  $\pi N$  and  $\eta N$  channels are so strongly coupled. Using the notation for the elastic  $T$ -matrix:

$$T_{\eta\eta}^{-1} + iq_{\eta} = 1/a + \frac{r_0}{2}q_{\eta}^2 + sq_{\eta}^4 \quad (1)$$

— with  $q_{\eta}$  being the momentum in the  $\eta N$  center-of-mass — resulted in the parameters  $a(\text{fm}) = 0.75(4) + i0.27(3)$ ,  $r_0(\text{fm}) = -1.50(13) - i0.24(4)$  and  $s(\text{fm}^3) = -0.10(2) - i0.01(1)$ . A later paper by the same authors [13] developed this formalism to include four explicit channels :  $\gamma N$ ,  $\pi N$ ,  $\pi\pi N$  and  $\eta N$  and new experimental data from GRAAL [29]. As indicated in Table I the scattering length was increased to  $a(\text{fm}) = 0.87(4) + i0.27(2)$  largely as a result of the new photoproduction data taken at higher energies. These large scattering lengths arise as an interplay of the attraction induced by the  $N(1535)$  state and an additional attractive interaction of unknown origin. These generate the  $\eta N$  threshold effect at the center-of-mass energy 1487.0 MeV. The threshold enhancement as seen in Fig. 1 is rather narrow on this energy scale. Details of this figure will be discussed later. This enhancement may dominate the physics of few-nucleon- $\eta$  systems, but it is not necessarily the case. The energy region that really matters covers a range of negative energies, which begins at the nucleon separation energy of about 10 MeV and extends down by approximately a further 10 MeV due to the recoil energy of  $N\eta$  pairs - making the center-of-mass energy of about 1460 MeV more relevant than the actual threshold energy of 1487.0 MeV. This point may be essential to understand a discrepancy between phenomenological  ${}^3\text{He} \eta$  scattering lengths and four-body calculations based on a plausible  $N\eta$  scattering amplitude. The phenomenological analysis — based upon elastic  $pd \rightarrow {}^3\text{He}\eta$  [23] and inelastic  $pd \rightarrow {}^3\text{He}\pi$  [30] reactions — produces  $A({}^3\text{He} \eta) = 4.24(29) + i0.72(81)$  fm, [31]. On a smaller data set a similar  $A({}^3\text{He} \eta) = |4.3(3)| + i0.5(5)$  fm is obtained in Ref. [32]. On the other

hand, a refined four-body calculation, [33], based on a  $N\eta$  scattering amplitude dominated by the  $N(1535)$  and fixed to  $a(fm) = 0.50 + i0.32$  fm finds  $A(^3He\ \eta) = 1.82 + i2.75$  fm. This difference in  $\text{Im}A(^3He\ \eta)$  indicates an uncertainty in the absorptive, subthreshold,  $N\eta$  scattering amplitude. Possible effects of the subthreshold region are also exemplified by calculations of the  $d\eta$  amplitude in Ref. [12]. Recent calculations of  $d\eta$  final state scattering performed in Ref. [22] indicate restrictions,  $0.42 < \text{Re}a(fm) < 0.72$  imposed by the experimental data. All these few-body calculations are obtained with the help of separable model extensions into the subthreshold region. In view of the complicated multichannel coupling to the  $N(1535)$  resonance, *e.g.* the effect of the  $N\eta$  threshold and also interference of the resonant and potential scattering, the subthreshold extrapolation from the scattering length value may be quite uncertain. Here, to provide amplitudes in this region one first uses the on-shell  $K$ -matrix approach. Next, the effective range expansion of on-shell amplitudes is calculated and off-shell amplitudes are generated by a simple separable model.

We recapitulate briefly the phenomenological model used to describe the  $S$ -wave interactions. The  $K$ -matrix is assumed to be of the form

$$K_{\alpha\beta} = B_{\alpha,\beta} + \sum_i \frac{\sqrt{\gamma_\alpha(i)\gamma_\beta(i)}}{E_i - E}, \quad (2)$$

where the sum  $i = 0, 1$  extends over the two states  $N(1535)$  and  $N(1650)$ . The  $E_i$  are the positions of poles that in a “conventional” model should be near the energies of the  $S$ -wave  $\pi N$  resonances  $N(1535)$  and  $N(1650)$ . The  $\gamma_\alpha(0, 1)$  are channel coupling parameters that are related to the widths of these resonances. Again these widths are thought to be more or less known, when data is analysed by a conventional model. However, less conventional models can lead to widths that are quite different [34]. Finally the  $B_{\alpha,\beta}$  are assumed, at first, to be energy independent background terms and are purely phenomenological. However, later we shall relax this by putting a theoretically motivated energy dependence into  $B_{\pi,\eta}$ . The list of free parameters contains 2 resonant energies, 5 couplings to the resonant states  $\gamma_\pi(0, 1)$ ,  $\gamma_\eta(0)$ ,  $\gamma_\gamma(0)$  and  $\gamma_3(0)$ . Here  $\gamma_3(0)$  describes small effects of the three body  $\pi\pi N$  channel. The additional 4 background parameters are  $B_{\eta,\eta}$ ,  $B_{\pi,\eta}$ ,  $B_{\gamma\eta}$ ,  $B_{\gamma\pi}$ . In comparison to the singular terms in Eq. (2), these background terms turn out to be very small with the exception of  $B_{\eta,\eta}$ , which generates a sizeable contribution to the value of the  $\eta N$  scattering length and the values of the scattering amplitudes at negative energies.

In this note, the calculation is extended to include the new Brookhaven Crystal Ball data for the  $\pi N \rightarrow \eta N$  cross section measured close to the  $\eta N$  threshold [35–37]. These now replace the ones from the review by Nefkens [26], used in Refs. [11,13], and also those earlier Brookhaven data from Refs. [4,38]. The latter were used by the present authors in Ref. [39] and gave rise to apparent massive uncertainties in the  $\eta N$  effective range parameters. In comparison to older measurements the new data offer better statistics, careful estimates of the systematic uncertainties and specified errors in pion beam momenta. An extension in the model involves an additional parameter  $\gamma_\eta(1)$  that couples the  $\eta N$  channel to  $N(1650)$ . Another improvement involves the background terms. These are due to cross-symmetric amplitudes<sup>1</sup> and potential interactions related to heavy meson exchanges and other unknown

---

<sup>1</sup>We wish to thank Professor U. Mosel for indicating this point.

mechanisms. On the phenomenological level there is no need to specify these explicitly. However, such mechanisms may induce some energy dependence to be accounted for. One expects the related effective range to result from the nearest singularities in the  $u, t$  channels. In the region of interest, extending from 100 MeV below up to 150 MeV above the  $\eta N$  threshold, it is the  $a_0$  meson exchange and  $u$ -channel nucleon pole that contribute to the effective range in the  $K$ -matrix. In view of the smallness of the  $N\eta N$  coupling constant these mechanisms are expected to contribute an effective range mainly in the crossing  $\pi, \eta$  transitions. The values of this range follow from the Born amplitudes describing the nearest singularities

$$V_{\pi,\eta} = \frac{C}{1 + Q^2/\Lambda(E)^2} , \quad (3)$$

where  $Q$  is a momentum transfer and  $C$  a constant. Projected onto  $S$ -waves such terms lead to logarithmic singularities for unphysical amplitudes. In our effective range expansion these unphysical singularities are represented by a pole. In the case of  $a_0$  meson exchange  $\Lambda = m_{a_0} \approx 5 \text{ fm}^{-1}$  and the nearest  $u$ -channel singularity, the nucleon pole, generates  $\Lambda \approx 3.5 \text{ fm}^{-1}$ . This sets the scale of effective range values. In terms of the parameter  $R$ , to be introduced later in Eq. (15), we obtain  $R_{\pi,\eta} \approx 1/\Lambda \approx 0.2 \text{ fm}$  as an order of magnitude estimate.

## II. THE CHOICE OF DATA AND RESULTS

Since the procedures followed in this current work are very similar to those found in Ref. [13], the interested reader should refer to that article for details concerning the fitting and error extraction. Also much of the data is the same as we used in previous analyses, namely,  $\pi N \rightarrow \pi N$  providing 23 data points in the center-of-mass energy range  $1369.2 \leq E_{\text{cm}} \leq 1705.0 \text{ MeV}$  [28],  $\gamma N \rightarrow \pi N$  16 data points with  $1352.0 \leq E_{\text{cm}} \leq 1546.3 \text{ MeV}$  [28] and  $\gamma N \rightarrow \eta N$  38 data points with  $1487.0 \leq E_{\text{cm}} \leq 1523.8 \text{ MeV}$  [29]. The new ingredient is the recent Brookhaven Crystal Ball data in Refs. [35–37]. These data are from two targets — hydrogen [35,36] and Polyethylene [37]. Both sets are consistent with each other, but here we use the latter, since there a more detailed discussion is made concerning uncertainties in the pion beam momentum. However, it should be added that the question of how the spread in the pion beam momentum affects the final value of the cross section is not yet fully resolved to the satisfaction of all the authors in Refs. [35–37]. Fortunately, as we shall see later, such refinements are not expected to change any of the conclusions arrived at in this paper. Therefore, for  $\pi N \rightarrow \eta N$  we use the 5 data points in the energy range  $1488.5 \leq E_{\text{cm}} \leq 1523.3 \text{ MeV}$  in Ref. [37]. These are shown in Table II. We give both the uncorrected  $\pi$ -beam momentum and that containing a correction suggested by the authors. Since there are uncertainties in arriving at such corrections, we check that our final results are not dependent on the precise values of the beam momenta. The errors quoted on the cross sections are the incoherent combination of the statistical and systematic errors given in Ref. [37].

Here we present several sets of results in Table III. The first set (A) fits all of the data given in the previous section using an energy independent form for describing the  $\pi N \rightarrow \eta N$  channel *i.e.*  $R_{\pi,\eta} = 0$  in Eq. (14) of the Appendix. The second set (B) fits the same data as

A but without the pion beam momentum correction in the  $\pi N \rightarrow \eta N$  data from Ref. [37] given in Table II. It is seen that the two sets have essentially the same effective range parameters. Furthermore, as seen in Fig. 1, the same is true for the  $\eta N \rightarrow \eta N$  amplitude away from the threshold. This means that, with the present data, the precise values of the  $\pi$ -beam momentum are not important for extracting this amplitude. However, the two sets give significantly different fits to the actual  $\pi N \rightarrow \eta N$  data as seen in Fig. 2. The fit to the beam corrected data is much better with a  $\chi^2/\text{dp}$  for these 5 data points being about 0.2 compared with the uncorrected value of about 1.8. However, the corresponding overall  $\chi^2/\text{dp}$  for the complete set of 121 data points are 1.01 versus 1.08.

As a further study of the importance of the new  $\pi N \rightarrow \eta N$  cross sections of Ref. [37], in set C we omit the Crystal Barrel data from set A. We see that, within the errors, the three complex parameters  $a$ ,  $r_0$  and  $s$  are unchanged. Also, as seen in Fig. 1 the  $\eta N$  amplitude is essentially unchanged. Therefore, one's first impression is that the new data of Refs. [35–37] adds little to our understanding of the  $\eta N \rightarrow \eta N$  amplitude. However, this is not true. Firstly, the error bars in set C are much larger than those in A *i.e.* the new data leads to tighter bounds on the  $\eta N$  amplitude. Secondly, the new data stabilizes the fit and makes it, as far as we can see, unique. We say this because the omission of the new data can lead to, at least, one other solution for the  $\eta N \rightarrow \eta N$  amplitude with a  $\chi^2/\text{dof}=1.054$  only slightly larger than the 1.045 of set C. This is shown as set D and is quite different to the earlier sets, but is rather similar to those extracted in Ref. [5] using a Lagrangian model — see Table I. However, it should be added that in Ref. [5] the authors basically use the  $\pi N \rightarrow \eta N$  data in Ref. [26], which reviews measurements made in the 1970's. These authors themselves point out that the data they are forced to use is poor. Furthermore, the new data is much nearer the  $\eta N$  threshold — the energy range that is most important for extracting the  $\eta N$  scattering parameters. The uncertainties that can arise when using poor  $\pi N \rightarrow \eta N$  data was noted earlier by the present authors in Ref. [39]. There we used some preliminary Brookhaven non-Crystal Ball data from experiment E909 [4,38]. This has now been superseded by the recent Crystal Ball data of Ref. [35–37]. In Ref. [39] we obtained one solution very similar to that in Ref. [11] quoted in Table I and a second solution  $a(\text{fm}) = 0.21 + i0.30$ ,  $r_0(\text{fm}) = -2.61 + i6.67$  and  $s(\text{fm}^3) = -0.39 - i3.67$ . This we called an "unconventional" solution in Ref. [39], since not only are *a etc* very different from before but also the form of the  $\eta N \rightarrow \eta N$  amplitude away from the threshold is qualitatively different. We have dwelt on this occurrence of unconventional solutions, since some of the scattering parameters in Table I could well be of this form. However, we want to emphasize that these unconventional solutions do not seem to arise in the present formulation using the complete data set as in A.

Sets E and F show the effect of removing the  $\gamma N \rightarrow \eta N$  data of Ref. [29]. In this case E is a conventional solution with a  $\chi^2/\text{dof}= 0.946$  and F an unconventional solution with an insignificantly smaller  $\chi^2/\text{dof}= 0.942$ . However, this solution has enormous error bars, so that the corresponding  $\eta N$  scattering parameters are very poorly determined.

Set G fits the same data as case A but now shows the effect of introducing an energy dependence into the basic  $\pi N \rightarrow \eta N$   $K$ -matrix element written in Eq. (14). The magnitude of the dependence is governed by the value of  $R_{\pi,\eta}$ . Here we take  $R_{\pi,\eta} = 0.2$  fm, a value suggested by theory — see the discussion after Eq. (3). This is seen to have a very small effect on the values of  $a$ ,  $r_0$  and  $s$  and also on the  $\chi^2/\text{dof}$ , reducing the latter from 1.0053

for case A to 1.0052. The reason for this is clear, since in the formalism the  $R_{\pi,\eta}$  always occurs in the combination  $R_{\pi,\eta}B_{\pi,\eta}$  and the minimization always produces a very small value  $B_{\pi,\eta} \sim 0.01$  fm. However, the errors on  $a$ ,  $r_0$  and  $s$  are now much larger than in case A indicating that this energy dependence is attempting to improve the data fit far away from the threshold. In fact, if — as a numerical experiment — the value of  $R_{\pi,\eta}$  is taken as a free parameter, then it becomes  $\sim 20$  fm — an unacceptably large value. This gives scattering parameters that are similar to set A, but away from the threshold the  $\eta N \rightarrow \eta N$  amplitude is qualitatively different. In particular, the  $\eta N \rightarrow \eta N$  develops a peak near 1400 MeV and an improvement in the fit to the  $\pi N \rightarrow \pi N$  results.

So far the emphasis has been on extracting the best values for the effective range parameters. This is certainly of interest when comparing different approaches as in Table I. However, as mentioned in the introduction, in practical applications involving systems with more than one nucleon, it is not the threshold value of the  $\eta N$  interaction that is relevant. Instead, depending on the multinucleon system, this interaction is needed over a range of energies upto 40 MeV below the threshold. In Fig. 1 the real and imaginary parts of the  $\eta N$  interaction are shown for sets A, B and C in Table III. There it is seen that both the real and imaginary parts are not only qualitatively but also quantitatively the same at all relevant energies and beyond.

### III. FITTING THE $\eta N \rightarrow \eta N$ AMPLITUDE WITH A SEPERABLE FORM

The requirement of few-body physics is a simple separable approximation to the off-shell  $\eta N \rightarrow \eta N$  amplitude. This we provide as

$$T_{\eta\eta}(q, E, q') = v_\eta(q)t_{\eta\eta}(E)v_\eta(q') \quad (4)$$

with  $v = 1/(1 + q^2\beta^2)$ , where  $\beta$  is the range parameter in this model, as discussed in Appendix. Now another effective range expansion is used for  $t_{\eta\eta}(E)$

$$t_{\eta\eta}(E)^{-1} + iq_\eta v(q_\eta)^2 = 1/a^s + \frac{r_0^s}{2}q_\eta^2 + s^s q_\eta^4. \quad (5)$$

This is to be compared with the corresponding expansion

$$T_{\eta\eta}^{-1} + iq_\eta = 1/a + \frac{r_0}{2}q_\eta^2 + s q_\eta^4 \quad (6)$$

defined in the introduction. The subthreshold amplitude required in few-body  $\eta$ -physics involves subthreshold energies  $E$  and physical momenta  $q$ . In contrast to  $T$  the subthreshold irregularities of  $t$  are removed in the large energy region.

The effective range expansions of both amplitudes lead to the algebraic relations

$$a^s = a; \quad r_0^s = r_0 - 4\beta^2/a; \quad s^s = s - r_0\beta^2 + 3\beta^4/a. \quad (7)$$

The range parameter  $\beta$  used in the separable model is not well determined. The actual value used ( $\beta = 0.31$  fm) is motivated by the two factors discussed after Eq. (3): the rough estimate of the  $N(1535)$  formfactor and the distance to the nearest singularities in the  $t$  and  $u$  channels .

## IV. CONCLUSION

In this paper we use a  $K$ -matrix method, developed earlier [11,13], to describe  $\pi N \rightarrow \pi N$ ,  $\pi N \rightarrow \eta N$ ,  $\gamma N \rightarrow \pi N$  and  $\gamma N \rightarrow \eta N$  data in an energy range of about 100 MeV or so each side of the  $\eta$ -threshold. Here the new feature is the incorporation of recent  $\gamma N \rightarrow \eta N$  near-threshold data [37] to replace that from the compilation of Ref. [26]. Eventhough this new data is not the main deciding factor for the actual values of the  $\eta$ -nucleon effective range scattering parameters  $a$ ,  $r_0$  and  $s$ , it does play an important role in determining the errors on these parameters. Furthermore, it appears to make set A in Table III the optimal unique solution. This is in contrast to earlier works, *e.g.* in Ref. [39], where other solutions appeared with very different values of  $a$ ,  $r_0$ ,  $s$  and forms of the  $\eta N$ -amplitude away from threshold. Our best and final value of  $a = 0.91(6) + i0.27(2)$  fm is large, but since the  $\eta N$ -amplitude drops rapidly below threshold — see Fig. 1 — it is not immediately clear whether it is sufficiently strong to develop quasi-bound states at the appropriate center-of-mass energies of upto to 40 MeV below the threshold. All that can be said is that the  $\eta N$ -amplitude at these subthreshold energies is not that small as to obviously eliminate the possibility of quasi-bound states. It could be that, in reality, the situation is borderline and so could explain why some theories [7,17–19,23] predict these states which, so far, are apparently not seen experimentally [20,24].

One of the authors (S.W.) wishes to acknowledge the hospitality of the Helsinki Institute of Physics, where part of this work was carried out. The authors also thank Drs. V. V. Abaev, B. Briscoe, D. Rebreyend, F. Renard and I. Strakovsky for useful correspondence and private discussions concerning their data. In addition the authors wish to thank Dr. N. Kelkar for pointing out misprints in Eq. 7. This project is financed by the Academy of Finland contract 54038, and the European Community Human potential Program HPRN-2002-00311 EURIDICE.

## APPENDIX

In this appendix, the physics of the above model is briefly presented. It is based on the nuclear resonance reaction theory of Wigner-Eisenbud. The spectrum of the system consists of channel states  $|i\rangle$  and an internal single baryon state  $|o\rangle$  of energy  $E_o$ . The latter may be a quark state or a bound state generated by some closed channels. The channel states interact via a potential  $V$  and the propagator for such a system is denoted by  $g_{i,j}$  in the channel sector, where  $g_{o,o} = (E - E_o)^{-1}$  and  $g_{i,o} = 0$ . Coupling of the channels to the internal state is generated by an additional interaction  $H$ , and the  $h_{i,o} = \langle o|H|i\rangle$  are coupling formfactors. The full propagator which involves both  $V$  and  $H$  is obtained from the equation

$$G = g + gHG. \quad (8)$$

The  $g$  already includes the  $V$  potential interactions and Eq. (8) is a separable equation easy to solve. This gives

$$G_{i,j} = g_{i,j} + f_{i,o} G_{o,o} f_{o,j} \quad (9)$$

$$G_{o,o} = (E - E_o - \Sigma_o)^{-1} ; G_{i,o} = g_{i,j} h_{j,o} G_{o,o}, \quad (10)$$

where  $\Sigma_o = h_{o,i}g_{i,i}h_{i,o}$  is the energy shift of the internal state due to the channel coupling and  $f_{i,o} = g_{i,j}h_{j,o}$ . In these, and the following equations, the summation over repeated channel indices and integration over corresponding momenta is understood.

The  $K$ -matrix is obtained in the standard way as  $K = UGU$  where  $G$  is the standing wave propagator and, in our extended space,  $U = V + H$ . This results in

$$K_{i,j} = K_{i,j}^{pot} + \gamma_{i,o}G_{o,o}\gamma_{o,j}, \quad (11)$$

where the potential part of the  $K$ -matrix is

$$K_{i,j}^{pot} = V_{i,j} + V_{i,m}g_{m,l}V_{l,j} \quad (12)$$

and the coupling formfactors become

$$\gamma_{i,o} = h_{i,o} + V_{i,m}g_{m,j}h_{j,o}. \quad (13)$$

The phenomenological model used in the main part of this work assumes  $\gamma_{i,o}$  to be constants and Eq. (11) is the basis of Eq. (2).

In our earlier work the  $K_{i,j}^{pot}$  have been considered to be the constants  $B_{i,j}^{pot}$ . Now this restriction is relaxed in the  $\pi\eta$  channel and the effective range expansion at the  $\eta N$  threshold is made in the standard way for the potential part

$$[K^{pot}(E)]_{\pi,\eta}^{-1} = [B]_{\pi,\eta}^{-1} + R_{\pi,\eta}q_\eta^2, \quad (14)$$

where the term  $B$  refers to the  $\eta$  threshold. As discussed in the text there are arguments to expect a range term in the  $\pi N$  to  $\eta N$  transition. Therefore, we invert Eq. (14) in the limited two channel space and obtain

$$K_{\pi,\pi}^{pot}(E) = \frac{B_{\pi,\pi}}{1 + 2\beta^2q_\eta^2 - \gamma q_\eta^4}, \quad K_{\eta,\eta}^{pot}(E) = \frac{B_{\eta,\eta}}{1 + 2\beta^2q_\eta^2 - \gamma q_\eta^4}, \quad K_{\pi,\eta}^{pot}(E) = \frac{B_{\pi,\eta} - DR_{\pi,\eta}q_\eta^2}{1 + 2\beta^2q_\eta^2 - \gamma q_\eta^4}, \quad (15)$$

where  $D = B_{\eta,\eta}B_{\pi,\pi} - B_{\pi,\eta}^2$ ,  $\beta^2 = B_{\pi,\eta}R_{\pi,\eta}$ ,  $\gamma = R_{\pi,\eta}^2D$  and  $q_\eta^2 = (E - E_{thr})2\mu_{N\eta}$ . For weak potentials parameter  $\beta$  is determined directly by the force range. Knowing  $K_{i,j}$ , the  $T_{i,j}$  are given by the usual relationship

$$K = \begin{pmatrix} K_{\pi,\pi} & K_{\eta,\pi} \\ K_{\pi,\eta} & K_{\eta,\eta} \end{pmatrix} \quad \text{and} \quad T = \begin{pmatrix} \frac{A_{\pi,\pi}}{1 - iq_\pi A_{\pi,\pi}} & \frac{A_{\eta,\pi}}{1 - iq_\eta A_{\eta,\eta}} \\ \frac{A_{\pi,\eta}}{1 - iq_\eta A_{\eta,\eta}} & \frac{A_{\eta,\eta}}{1 - iq_\eta A_{\eta,\eta}} \end{pmatrix}, \quad (16)$$

where  $q_{\pi,\eta}$  are the center-of-mass momenta of the two mesons in the two channels  $\pi, \eta$ . The channel scattering lengths  $A_{i,j}$  are expressed in terms of the  $K$ -matrix elements as

$$A_{\pi,\pi} = K_{\pi,\pi} + iK_{\pi,\eta}^2q_\eta/(1 - iq_\eta K_{\eta,\eta}), \quad A_{\eta,\pi} = K_{\eta,\pi}/(1 - iq_\pi K_{\pi,\pi}), \\ A_{\eta,\eta} = K_{\eta,\eta} + iK_{\eta,\pi}^2q_\pi/(1 - iq_\pi K_{\pi,\pi}). \quad (17)$$



## REFERENCES

- [1] C. Bennhold and H. Tanabe, Nucl. Phys. **A350**, 625 (1991).
- [2] R. S. Bhalerao and L. C. Liu, Phys. Rev. Lett. **54**, 865 (1985).
- [3] V. Yu. Grishina, L. A. Kondratyuk, M. Buscher, C. Hanhart, J. Haidenbauer and J. Speth, Phys. Lett. **B475**, 9 (2000) and nucl-th/9905049.
- [4] W. Briscoe, T. Morrison, I. Strakovsky and A.B. Gridniev,  $\pi$ -N newsletter **16**, 391 (2002).
- [5] T. Feuster and U. Mosel, Phys. Rev. C **58**, 457 (1998).
- [6] Ch. Sauerma, B.L. Friman and W. Nörenberg, Phys. Lett. B **341**, 261 (1995).  
Ch. Deutsch-Sauerma, B.L. Friman and W. Nörenberg, " $\eta$ -meson photoproduction off protons and deuterons", nucl-th/9701022.
- [7] C. Wilkin, Phys. Rev. C **47**, R938 (1993).
- [8] V.V. Abaev and B.M.K. Nefkens, Phys. Rev. C **53**, 385 (1996).
- [9] N. Kaiser, P.B. Siegel and W. Weise, Phys. Lett. B **362**, 23 (1995).
- [10] M. Batinić, I. Dadić, I. Šlaus, A. Švarc, B. M. K. Nefkens and T.-S. H. Lee, "Update of the  $\pi N \rightarrow \eta N$  and  $\eta N \rightarrow \eta N$  partial-wave amplitudes", nucl-th/9703023.
- [11] A. M. Green and S. Wycech, Phys. Rev. C **55** (1997)R2167 and nucl-th/9703009.
- [12] S. A. Rakityansky, S. A. Sofianos, N. V. Shevchenko, V. B. Belyaev, W. Sandhas, Nucl. Phys. **A684**, 383 (2001).
- [13] A. M. Green and S. Wycech, Phys. Rev. C **60** (1999) 035208 and nucl-th/9905011.
- [14] M. Batinić, I. Šlaus, A. Švarc and B.M.K. Nefkens, Phys. Rev. C **51**, 2310 (1995) and erratum Phys. Rev. C **57**, 1004 (1998).
- [15] M. Arima, K. Shimizu and K. Yazaki, Nucl. Phys. **A543**, 613 (1992).
- [16] G. Penner and U. Mosel, Phys. Rev. C **66**, 055212 (2002).
- [17] Q. Haider and L.C. Liu, Phys. Lett. B **172**, 257 (1986),  
L.C. Liu and Q. Haider, Phys. Rev. C **34**, 1845 (1986).
- [18] G. L. Li, W. K. Cheung and T. T. Kuo, Phys. Lett. B **195**, 515 (1987).
- [19] T. Ueda, Phys. Rev. Lett. **66**, 297 (1991).
- [20] H. Calén *et al.*, Phys. Rev. Lett. **80**, 2069 (1998).
- [21] S. Wycech and A. M. Green, Phys. Rev. C **64**, 045206 (2001).
- [22] H. Garcilazo and M. T. Peña, Phys. Rev. C **66**, 034606 (2002) and nucl-th/0406070.
- [23] B. Mayer *et al.*, Phys. Rev. C **53**, 2068 (1996).
- [24] R. E. Chrien *et al.*, Phys. Rev. Lett. **60**, 2595 (1988).
- [25] R. S. Hayano, S. Hirenzaki and A. Gillitzer, Eur.Phys.J.A **6**, 99 (1999) and nucl-th/9806012.
- [26] M. Clajus and B. M. K. Nefkens,  $\pi$ -N newsletter **7**, 76 (1992).
- [27] B. Krusche *et al.*, Phys. Rev. Lett. **74**, 3736 (1995).
- [28] R. A. Arndt, J. M. Ford and L. D. Roper, Phys. Rev. D **32**, 1085 (1985).
- [29] F. Renard, private communication, F. Renard *et al.*, Phys. Lett. B **528**, 215 (2002).
- [30] M. Abdel-Bary *et al.*, Phys. Rev. C **68**, 021603(R) 2003.
- [31] A. M. Green and S. Wycech, Phys. Rev. C **68**, 061601(R) (2003).
- [32] A. Sibirtsev, J. Haidenbauer, C. Hanhart and J. A. Niskanen, "The  $^3\text{He}\eta$  scattering length revisited", to be published in the Eur. Phys. J. A and nucl-th/0310079.
- [33] A. Fix and H. Arenhovel, Phys. Rev. C **68**, 044002 (2003).

- [34] R. A. Arndt, A. M. Green, R. L. Workman and S. Wycech, Phys. Rev. C **58**, 3636 (1998) and nucl-th/9807009.
- [35] N. G. Kozlenko, Acta Phys. Polon. B **31**, 2239 (2000).
- [36] N. G. Kozlenko *et al.*, Phys. of Atom. Nuclei **66**, 110 (2003).
- [37] N. G. Kozlenko *et al.*, “Measurements of the Total and Differential Cross Sections of the Reaction  $\pi^-p \rightarrow \eta n$  using the Polyethylene Target and the Crystal Ball Detector”, Gatchina preprint 2542 (2003).
- [38] T. Morrison, PhD. thesis George Washington University.
- [39] A. M. Green and S. Wycech, “Uncertainties in the  $\eta$ -Nucleon Scattering Length and Effective Range”, nucl-th/0009053.

# TABLES

TABLE I. A selection of  $\eta N$ - scattering lengths and effective ranges appearing in the literature.

Reaction or Method	Scattering Length(fm)	Effective range (fm)
[1]	$0.25+i0.16$	
[2]	$0.27+i0.22$	
$pn \rightarrow d\eta$ [3]	$\leq 0.3$	
[4]	$0.46(9)+i0.18(3)$	
[5]	$0.487+i0.171$	$-6.060-i0.177$
[6]	$0.51+i0.21$	
[7]	$0.55(20)+i0.30$	
[5]	$0.577+i0.216$	$-2.807-i0.057$
[8]	$0.621(40)+i0.306(34)$	
[9]	$0.68+i0.24$	
[10]	$0.717(30)+i0.263(25)$	
Coupled $K$ -matrices [11]	$0.75(4)+i0.27(3)$	$-1.50(13)-i0.24(4)$
$\eta d \rightarrow \eta d$ [12]	$\geq 0.75$	
Coupled $K$ -matrices [13]	$0.87+i0.27$	
[14]	$0.91(3)+i0.29(4)$	
[15]	$0.980+i0.37$	
[16]	$0.991+i0.347$	$-2.081-i0.81$
Coupled $K$ -matrices [13]	$1.05+i0.27$	

TABLE II. The  $\pi N \rightarrow \eta N$  data from Ref. [37]. The uncorrected  $\pi$ -beam momentum is denoted by [UC] and the corrected momentum by [C].

$P_\pi$ MeV/c [UC]	$P_\pi$ MeV/c [C]	$\sigma$ mb
692.5	687.1	0.64(17)
702.4	701.0	1.73(15)
714.5	713.1	2.13(15)
732.1	731.6	2.69(20)
744.3	744.1	2.68(20)

TABLE III. The effective range parameters  $a$ ,  $r_0$  and  $s$  using the notation for the elastic  $T$ -matrix:  $T_{\eta\eta}^{-1} + iq_\eta = 1/a + \frac{r_0}{2}q_\eta^2 + sq_\eta^4$ , – with  $q_\eta$  being the momentum in the  $\eta N$  center-of-mass. Sets A and B fit all the data, with A using the corrected  $\pi$ -beam momentum in Table II and B without this correction. Set C omits the  $\pi N \rightarrow \eta N$  data of Ref. [37]. Set D is a second but unconventional solution when the data of Ref. [37] is omitted. Set E omits the  $\gamma N \rightarrow \eta N$  data of Ref. [29]. Set F is a second but unconventional solution when the data of Ref. [29] is omitted. Set G fits the same data as Set A but with an energy dependence included in the  $\pi N \rightarrow \eta N$   $K$ -matrix element of Eq. 14.

Set	Re $a$	Im $a$	Re $r_0$	Im $r_0$	Re $s$	Im $s$
A	0.91(6)	0.27(2)	−1.33(15)	−0.30(2)	−0.15(1)	−0.04(1)
B	0.88(5)	0.25(2)	−1.37(16)	−0.31(2)	−0.15(1)	−0.04(1)
C	0.93(21)	0.27(10)	−1.3(6)	−0.31(7)	−0.16(7)	−0.05(3)
D	0.51(9)	0.26(3)	−2.5(6)	0.3(5)	0.2(2)	−0.0(1)
E	0.77(9)	0.25(5)	−1.8(4)	−0.3(1)	−0.10(69)	−0.02(3)
F	0.4(5)	0.3(2)	−4(20)	2(5)	—	—
G	0.92(20)	0.27(9)	−1.3(6)	−0.30(6)	−0.15(6)	−0.04(3)

# FIGURES

FIG. 1. The real(R) and imaginary(I) parts of the  $T(\eta\text{-}N)$  scattering amplitude. The solid(dashed) lines show the fit with(without) the pion beam correction of the  $\pi N \rightarrow \eta N$  data from Ref. [37] — see Table II. The dotted lines show the effect of not including this  $\pi N \rightarrow \eta N$  data in the fit. All three sets of curves are more or less indistinguishable.

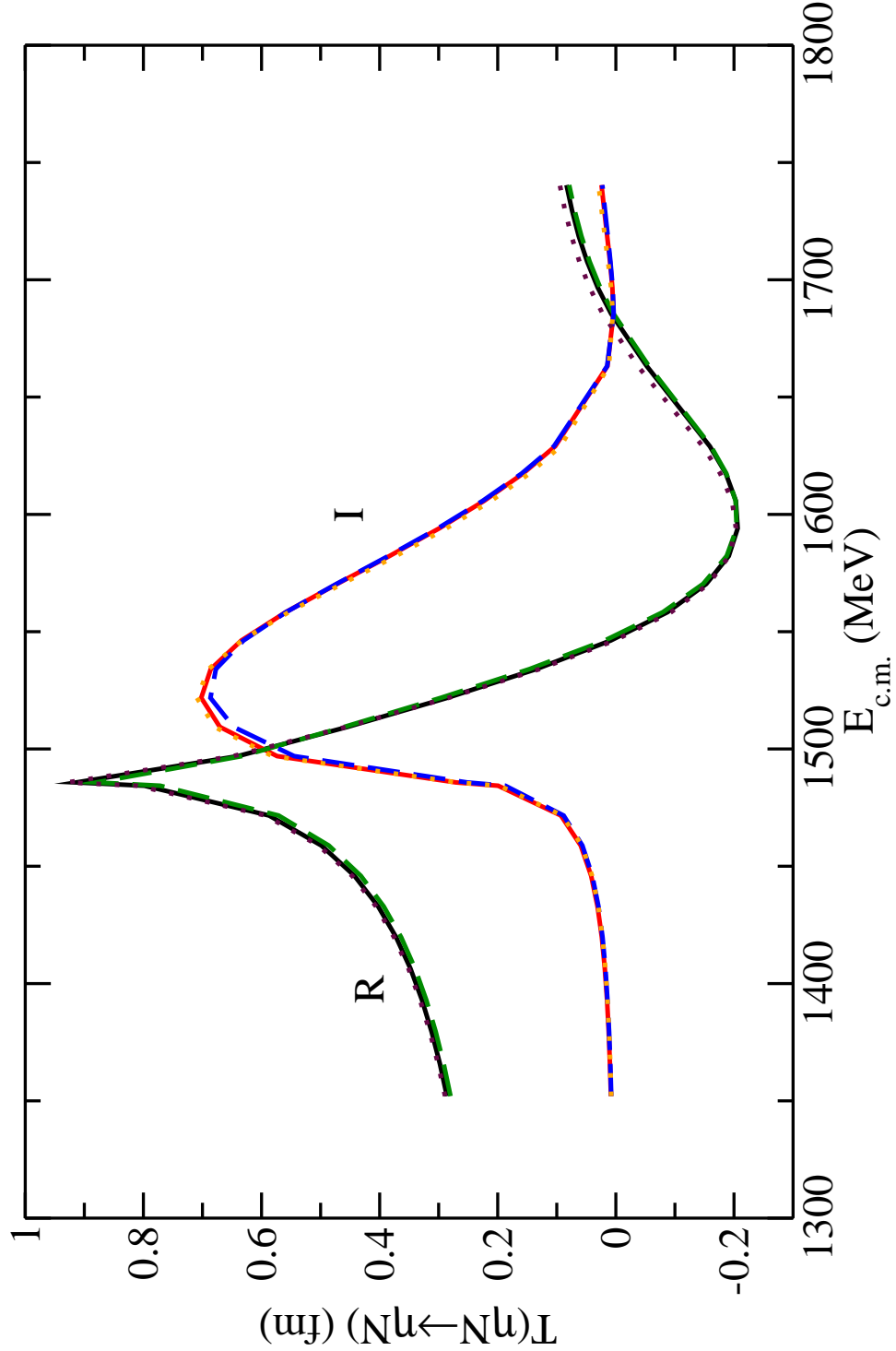


FIG. 2. Fits to the  $\pi N \rightarrow \eta N$  data from Ref. [37] with (solid line) and without (dashed line) the  $\pi$ -beam correction. The squares are for the uncorrected  $\pi$ -beam momenta and the circles for the corrected momenta — see Table II.

